

# DEEP JOINT TRANSMISSION-RECOGNITION FOR POWER-CONSTRAINED IOT DEVICES

Mikolaj Jankowski, Deniz Gündüz, Krystian Mikolajczyk  
Imperial College London

{mikolaj.jankowski17, d.gunduz, k.mikolajczyk}@imperial.ac.uk

## Abstract

We propose a joint transmission-recognition scheme for efficient inference at the wireless network edge. Our scheme allows for reliable image recognition over wireless channels with significant computational load reduction at the sender side. We incorporate recently proposed deep joint source-channel coding (JSCC) scheme, and combine it with novel filter pruning strategies aimed at reducing the redundant complexity from neural networks. We evaluate our approach on a classification task, and show satisfactory results in both transmission reliability and workload reduction. This is the first work that combines deep JSCC with network pruning and applies it to images classification over wireless network.

*Index Terms*— Joint source-channel coding, image classification, IoT, pruning, deep learning

## 1 Introduction

Number of Internet of Things (IoT) devices reached 22 billion at the end of 2018 and is expected to grow up to 75 billion by the end of 2025 [1]. IoT devices are already present in almost every area within industry, business, and everyday life, where they have been successfully deployed for measurement and monitoring tasks. Currently, most IoT devices act as wireless sensors that collect data and offload it to a cloud or edge server for further processing. This creates a major bottleneck in many emerging IoT applications as communication consumes significant energy and introduces latency.

In this work, we consider deep neural network (DNN) based inference by a power-constrained edge device. Due to the stringent power and memory constraints, the device cannot perform all the computations required by a complex DNN architecture. For example, a single forward pass of the ResNet-152 [2] architecture, given input image of  $224 \times 224$  resolution, requires  $11 \times 10^9$  floating-point operations (FLOPs), which requires a few minutes of computing on simple IoT devices, which are usually limited to a few MFLOPs per second. We assume that an edge server is available to help the device to perform the inference task. The opposite extreme to local computing would be to offload all the data to the edge server, where a DNN of any complexity can be deployed. Note, however, that parts of the data that the device is sending may not be useful for the underlying task. An alternative approach is to preprocess the data on the edge device, within the available computational limits, and transmit the resulting features to the edge server. We therefore encounter two main challenges: minimizing the number of computations that have to be done locally, and designing a robust communication scheme within the limited available transmission power.

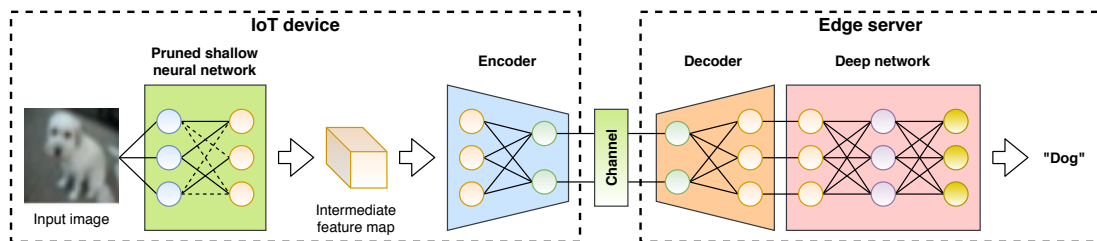


Figure 1: An overview of the proposed system. The baseline neural network is split between an IoT device and an edge server. Given an input image, pruned sub-network performs the first part of the forward pass to generate an intermediate feature map, which is then compressed by an autoencoder and sent through a wireless link. At the receiver side, the compressed feature map is decoded and the remaining part of the forward pass is completed to obtain the final prediction.

To address the first challenge, DNNs architectures that operate within the low-complexity constraints of mobile devices are proposed in [3]. These may still need hundreds of millions floating-point operations (FLOPs) to perform a single forward-pass, which may be unacceptable for certain IoT devices. Some recent works [4, 5, 6] suggest splitting DNNs into two parts, where the first part meets the computational limitations of the IoT device, while the second part is deployed on the edge server. This approach then requires reliable transmission of the intermediate feature vectors output by the first part of the DNN to the edge server. A typical approach is to quantize these feature vectors, and transmit them over the channel using a digital channel code [4, 5]. These methods consider the amount of information (e.g., the number of bits) that must be transmitted to the edge server, but ignore the energy and latency cost of communications. Moreover, reliable transmission of the feature vectors over a wireless channel requires an accurate estimate of the channel state at the edge device, and separate compression and channel coding is known to be suboptimal under strict delay constraints. Recently, DNN-based JSCC scheme has been shown to provide improved performance and robustness in wireless image transmission [7, 8, 9]. Deep JSCC schemes have also been applied in distributed inference scenarios [10, 6, 11], but they require a significant number of on-device computations to run a forward pass of the underlying DNN.

In this work, we propose to reduce the on-device computational load by incorporating a pruning step in the network training. Network pruning [12] aims at reducing the computational redundancy within DNNs by efficiently removing certain neurons, convolutional filters or entire layers based on a saliency measure or a regularization term. Therefore, given a certain channel condition and computational power constraints, our goal is to find the optimal DNN splitting point and the pruning parameters to ensure the best possible accuracy as well as efficiency in a given scenario. In particular, we focus on image classification as one of the most frequent tasks performed to analyse image content. Network splitting together with pruning for edge devices has recently been studied in [13] considering separate source and channel coding. In contrast, our work is the first to study deep joint source-channel coding combined with pruning for power-constrained IoT devices. Our contributions can be summarized as follows:

- We propose a DNN training procedure for joint device-edge inference systems under extreme power and latency constraints by combining novel pruning and splitting techniques with deep JSCC.
- We propose an autoencoder-based network for intermediate feature maps compression to

allow for bandwidth reduction.

- We provide an extensive evaluation of the proposed approach at various DNN splitting points, different channel SNRs, bandwidth and computational power constraints.

## 2 Methods

In this work we propose a 4-step training strategy for combining partial network pruning with deep JSCC for transmitting feature maps output by an arbitrary hidden layer of the network (Fig. 1). Such approach allows for a reduction in both the computational power required at the IoT device and the communication overhead. Most popular convolutional neural networks (CNNs), such as VGG [14] or ResNet [2] perform spatial dimensionality reduction of intermediate feature maps by applying pooling operations or convolutional filters with stride greater than 1. Nevertheless, as spatial dimension is being reduced, number of channels is usually expanded to extract the most significant features from the input image. Therefore, in the first few layers of such networks, the total dimensionality of the feature map increases up to a certain point, after which it starts to decrease due to further downsamplings. As a consequence, there exists a hidden layer within such network, where the size of the intermediate feature map becomes lower than the size of the input image. Transmitting such a feature map instead of the original image, is beneficial in terms of required bandwidth, but increases the computational power required to preprocess the image as more layers have to be computed on the device. This defines a trade-off between on-device computation and communication overhead, which we aim to optimize.

### 2.1 Channel model

In this work we consider an additive white Gaussian noise (AWGN) channel, but any differentiable channel model can be employed instead. Specifically, given a channel input vector  $\mathbf{x} \in \mathbb{R}^B$ , where  $B$  is the vector's length, the channel output  $\mathbf{y} \in \mathbb{R}^B$  can be calculated as  $\mathbf{y} = \mathbf{x} + \mathbf{z}$ , where  $\mathbf{z}$  is a noise vector containing elements  $z \sim \mathcal{N}(0, \sigma^2)$ . Before generating the output  $\mathbf{y}$  we first normalize each vector  $\mathbf{x}$  to meet the average power constraint of  $P = 1$ , i.e.,  $\frac{1}{B} \sum_{i=1}^B x_i^2 \leq P$ . We evaluate the recognition accuracy for different channel signal-to-noise ratios (SNRs) given by  $\frac{P}{\sigma^2}$ . To compare our JSCC approach to digital methods we use standard Shannon capacity formula given by  $C = \frac{1}{2} \log_2 \left( 1 + \frac{P}{\sigma^2} \right)$ .

### 2.2 Classification baseline

Our framework is flexible, and can be easily adapted to any system that incorporates DNNs. We focus on image classification task as it is the most frequent approach to automatically analyse image content and generate its metadata. Given an image and a finite set of possible classes, the classification task aims at assigning the correct class label to the image. We experiment with VGG16 [14] with batch normalization (BN) added after each convolutional layer as it is one of the most popular networks employed for image classification. The network consists of 13 convolutional layers with stride 1 divided into 5 blocks, where each block is followed by a pooling operation. We consider each of the pooling operations as a potential network splitting point as it provides feature compression by construction, and does not affect the accuracy. After the last pooling layer we also employ a fully-connected classifier consisting of three fully-connected layers, where the first two have the output size of 512 and the last one maps 512-dimensional vector to 100-dimensional class predictions.

### 2.3 Autoencoder architecture

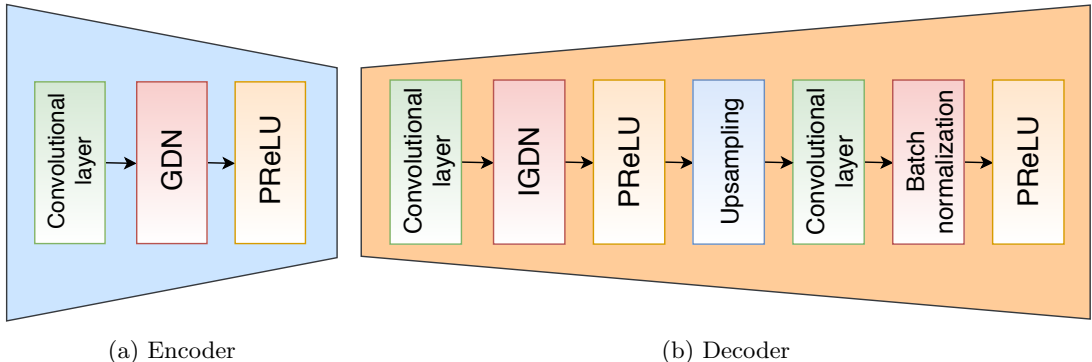


Figure 2: Proposed encoder and decoder architectures for the JSCC scheme. At the encoder, dimensionality reduction is performed by the convolutional layer. Shallow structure of the encoder reduces the computational load on the power-constrained device.

In order to compress feature maps and reduce communication requirements, we employ an autoencoder shown in Fig. 2. Its asymmetrical structure is designed to reduce on-device computations, therefore the encoder’s architecture (Fig. 2a) consists of a single convolutional layer of stride  $2 \times 2$  and  $3 \times 3$  kernels, which perform both spatial and channel-wise compression of the feature map in a single step. The convolutional layer is followed by the generalized divisive normalization (GDN) layer [15], which is commonly used in most successful deep compression schemes such as [16] as a replacement of BN. GDN operation is defined as:

$$u_i^{(k+1)}(m, n) = \frac{w_i^{(k)}(m, n)}{\left(\beta_{k,i} + \sum_j \gamma_{k,ij} \left(w_j^{(k)}(m, n)\right)^2\right)^{\frac{1}{2}}}, \quad (1)$$

where  $u_i^{(k)}(m, n)$  denotes the  $i$ th output channel of the  $k$ th stage of the encoder at the spatial location  $(m, n)$  and  $w_i^{(k)}(m, n)$  denotes the corresponding input value. The approximate inverse operation, called IGDN is given by:

$$\hat{w}_i^{(k+1)}(m, n) = \hat{u}_i^{(k)}(m, n) \left(\hat{\beta}_{k,i} + \sum_j \hat{\gamma}_{k,ij} \left(\hat{u}_j^{(k)}(m, n)\right)^2\right)^{\frac{1}{2}}, \quad (2)$$

where  $\hat{w}$  denotes the output and  $\hat{u}$  the corresponding input to IGDN.

Finally, we employ parametric rectified linear unit (PReLU) [17] as an activation function to further increase the learning capacity of our model.

In the decoder (Fig. 2b) we first perform a single convolution with stride  $1 \times 1$  and  $3 \times 3$  kernel size on the compressed feature map as we expect it to learn channel characteristics and introduce denoising. Convolutional layer is followed by IGDN operation, PReLU activation and upsampling that restores the original spatial dimensionality of the intermediate feature map. Finally, another convolutional layer with the same stride and kernel size is applied to increase feature map’s depth to its original value, followed by BN and PReLU. Please note that the number of channels effectively controls the size of the transmitted vector as our encoder always reduces the spatial dimensionality by a factor of 4. The only exception is the last block of VGG16 network (after pooling 5), where the feature map of size  $1 \times 1 \times 512$  cannot be downsampled so we keep the spatial dimensions the same, varying only the number of channels.

## 2.4 Training strategy

Our training strategy consists of 4 steps. Firstly, we pretrain the VGG16 network with cross-entropy loss for 60 epochs, using SGD [18] optimizer with learning rate of 0.01, momentum of 0.9, and  $L_2$  penalty on network parameters weighted by  $5 \cdot 10^{-4}$  to avoid overfitting. We reduce the learning rate by a factor of 0.1 after 20th and 40th epochs.

Next, we select the splitting point after one of the pooling layers of the network and employ network pruning. In our work we follow the pruning algorithm from [19], which uses Taylor expansion to approximate the change in the loss function induced by pruning the network parameters. In principle, the algorithm evaluates the importance of each convolutional filter up to the splitting point and removes the least significant ones. In our setup, the algorithm reduces 512 convolutional filters at a single pruning iteration, followed by additional 10 training epochs with learning rate of 0.0001 to recover the accuracy lost by filter removal.

After pruning is completed, we run a forward pass through the pruned part of the network with each image in the training set to extract all the possible feature maps at the splitting point. We use the feature maps as a new training set for our autoencoder, which we pretrain for 40 epochs with learning rate of 0.1, momentum of 0.9 and  $L_2$  penalty weighted by  $5 \cdot 10^{-4}$ . We use  $L_1$ -loss to recover the feature maps as close to their original versions as possible. This step is crucial to speed-up the convergence of the end-to-end training; since the feature maps are low-dimensional and autoencoder architecture is very simple, its execution is relatively fast. Starting from this step, we incorporate an AWGN channel model between the encoder and decoder to learn robustness against channel noise.

In the last step we perform end-to-end training of the entire network. Specifically, we combine both parts of the VGG16 network and place pretrained autoencoder at the splitting point. Similarly to the first step, we train the network with cross-entropy loss, SGD optimizer with learning rate of 0.0001 and the other parameters unchanged.

## 3 Results

In this section we evaluate the performance of the proposed approach and compare it with other schemes, both analog and digital. Before presenting the results, we will first discuss the experimental setup.

### 3.1 Experimental setup

In order to measure the accuracy of the proposed method in image classification, we employ popular CIFAR100 dataset [20]. The dataset consists of 60000 RGB images divided into 100 different classes (e.g., bicycle, fox, oranges etc.). Each class is represented evenly by 600 images, 500 for training and 100 for testing. Original resolution of the images is  $32 \times 32$  pixels. During training, we first perform common data augmentation steps, namely we apply 4 pixels zero-padding at each side of an image and randomly crop  $32 \times 32$  pixel tiles. Moreover, we randomly flip images horizontally with a probability of 50% and normalize them to have zero mean and unit variance. After such preprocessing, we perform multiple trainings of the proposed system, according to the strategy presented in Section 2.4 for different values of channel SNR, pruning ratios, network splits and channel bandwidths, and evaluate the corresponding classification accuracy and required number of computations. In order to calculate computational complexity of our approach, we count the number of FLOPs necessary to perform a single forward pass of the layers executed at the edge device (pruned shallow sub-network and the encoder).

### 3.2 Channel bandwidth and on-device computation

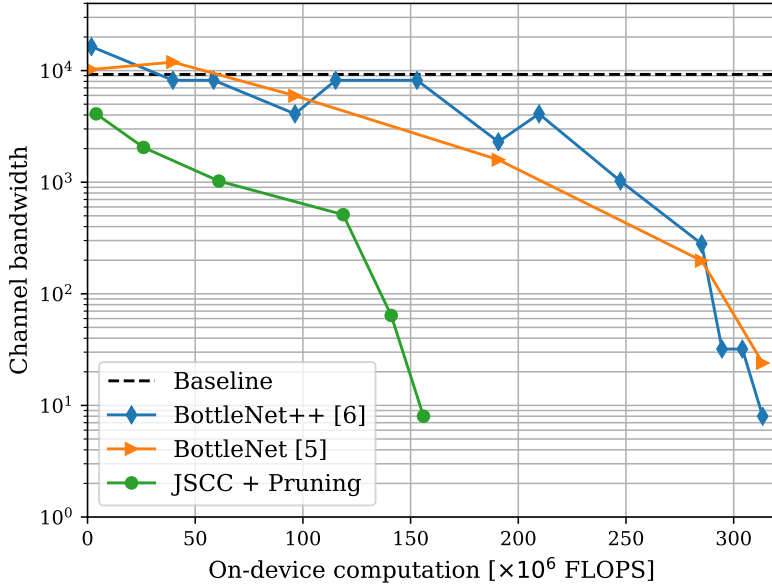


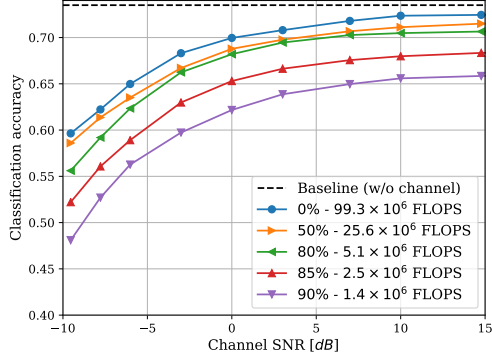
Figure 3: Channel bandwidth as a function of on-device computation. The accuracy remains within 2% from the classification baseline.

In this section we select the models that minimize the channel bandwidth, which we define as the number of real symbols transmitted per channel use, and maximize the pruning ratio (which results in minimal on-device computation), under channel SNR of 14.5dB, allowing for a maximum drop of 2% into the classification accuracy compared to the baseline. Results in Fig. 3 clearly show that our proposed approach beats both the JSCC-based and the digital communication schemes by a large margin. Within very limited computational resources, which corresponds to strict bandwidth and latency constraints that are common in IoT applications, proposed scheme requires only  $4 \times 10^6$  FLOPs to achieve approximately  $3 \times$  bandwidth reduction compared to the *baseline*, which we define as transmitting the original PNG image and performing classification on the edge server without any processing at the edge device.

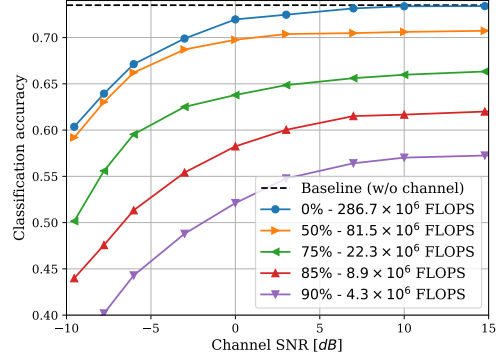
Another superiority of our approach is that achieving  $64 \times$  bandwidth reduction (from 512 symbols to 8 symbols) after the last pooling in VGG16 network is possible with only  $156 \times 10^6$  FLOPs, which is only half of the operations necessary to run a single forward pass of the unpruned network. More importantly, given  $156 \times 10^6$  FLOPs limitation, which is the number of operations that can be performed on a single Apple Watch device within 0.05s, we achieve  $1024 \times$  bandwidth reduction compared to [6].

### 3.3 Comparison between different pruning ratios

In this section we evaluate the influence of different pruning ratios on classification accuracy under different channel SNRs for fixed splitting points and available channel bandwidths (Fig.



(a)  $B = 2048$ , splitting after pooling 2



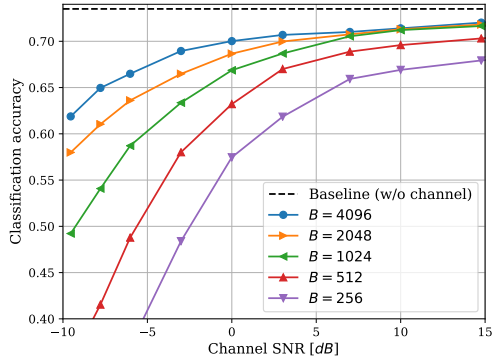
(b)  $B = 128$ , splitting after pooling 4

Figure 4: Classification accuracy as a function of the channel SNR for different pruning ratios and channel bandwidth fixed to  $B$ .

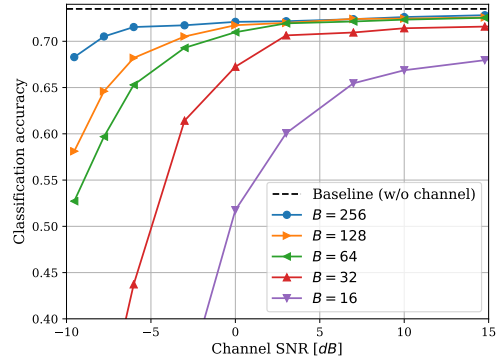
4a and Fig. 4b).

It is clear, that pruning leads to a drop in accuracy, as expected. Nevertheless, given reasonable pruning ratios of up to 50%, accuracy drop decreases as we approach very low values of channel SNR. This behaviour may stem from the fact that feature distortion caused by network pruning becomes less significant when the channel is very noisy. Another important observation is that very high pruning ratios do not seem to reduce nor improve the robustness of the communication scheme - the accuracy drop caused by reducing the channel SNR follows a similar trend for every pruning ratio considered in this experiment.

### 3.4 Comparison between different channel bandwidths



(a) Splitting after pooling 2 with pruning ratio of 0.5 ( $24.3 \times 10^6$  FLOPs)



(b) Splitting after pooling 4 with pruning ratio of 0.25 ( $160.2 \times 10^6$  FLOPs)

Figure 5: Classification accuracy as a function of the channel SNR for different channel bandwidths.

In our last experiment, we fix the pruning ratios and the splitting points and examine the influence of the available bandwidth on the classification accuracy under different channel SNR values (Fig. 5a and Fig. 5b).

One can clearly see that the available bandwidth is a crucial factor in the performance. In both experiments, reducing the bandwidth produced similar results under high channel SNR values. Nevertheless, as channel condition gets worse, the more limited the available bandwidth is, the sharper the drop in the accuracy with channel SNR.

## 4 Conclusions

In this work we studied image classification at the wireless network edge considering a power and bandwidth limited edge device. We proposed a novel method to minimize the IoT device computational load taking into account both the classification and communication aspects, under a constraint on the available bandwidth. Our approach achieves superior results in classification accuracy even with extremely limited computational and communication resources. This is achieved by a multiple-step combination of novel deep JSCC with additional pruning.

In order to further develop this design, we plan to reduce the number of training steps by incorporating pruning into the joint training phase. We will also aim at designing communication-aware pruning, that not only reduces the computational complexity, but its filter saliency measure is directly based on the wireless channel condition.

## References

- [1] S. Lucero. (2016, Mar.) Iot platforms: enabling the internet of things. [Online]. Available: <https://cdn.ihs.com/www/pdf/enabling-IOT.pdf>
- [2] K. He, X. Zhang, S. Ren, and J. Sun, "Deep residual learning for image recognition," in *Proceedings of the IEEE conference on computer vision and pattern recognition*, 2016, pp. 770–778.
- [3] A. G. Howard, M. Zhu, B. Chen, D. Kalenichenko, W. Wang, T. Weyand, M. Andreetto, and H. Adam, "Mobilenets: Efficient convolutional neural networks for mobile vision applications," *arXiv preprint arXiv:1704.04861*, 2017.
- [4] H. Li, C. Hu, J. Jiang, Z. Wang, Y. Wen, and W. Zhu, "Jalad: Joint accuracy-and latency-aware deep structure decoupling for edge-cloud execution," in *2018 IEEE 24th International Conference on Parallel and Distributed Systems (ICPADS)*. IEEE, 2018, pp. 671–678.
- [5] A. E. Eshratifar, A. Esmaili, and M. Pedram, "Bottlenet: A deep learning architecture for intelligent mobile cloud computing services," in *2019 IEEE/ACM International Symposium on Low Power Electronics and Design (ISLPED)*. IEEE, 2019, pp. 1–6.
- [6] J. Shao and J. Zhang, "Bottlenet++: An end-to-end approach for feature compression in device-edge co-inference systems," *arXiv preprint arXiv:1910.14315*, 2019.
- [7] E. Bourtsoulatze, D. B. Kurka, and D. Gündüz, "Deep joint source-channel coding for wireless image transmission," *IEEE Transactions on Cognitive Communications and Networking*, vol. 5, no. 3, pp. 567–579, 2019.



- [8] D. B. Kurka and D. Gündüz, “Successive refinement of images with deep joint source-channel coding,” in *2019 IEEE 20th International Workshop on Signal Processing Advances in Wireless Communications (SPAWC)*, July 2019, pp. 1–5.
- [9] D. B. Kurka and D. Gündüz, “Deepjscc-f: Deep joint-source channel coding of images with feedback,” 2019.
- [10] C. Lee, J. Lin, P. Chen, and Y. Chang, “Deep learning-constructed joint transmission-recognition for internet of things,” *IEEE Access*, vol. 7, pp. 76 547–76 561, 2019.
- [11] M. Jankowski, D. Gündüz, and K. Mikolajczyk, “Deep joint source-channel coding for wireless image retrieval,” *arXiv preprint arXiv:1910.12703*, 2019.
- [12] Y. LeCun, J. S. Denker, and S. A. Solla, “Optimal brain damage,” in *Advances in Neural Information Processing Systems 2*, D. S. Touretzky, Ed. Morgan-Kaufmann, 1990, pp. 598–605. [Online]. Available: <http://papers.nips.cc/paper/250-optimal-brain-damage.pdf>
- [13] W. Shi, Y. Hou, S. Zhou, Z. Niu, Y. Zhang, and L. Geng, “Improving device-edge cooperative inference of deep learning via 2-step pruning,” *arXiv preprint arXiv:1903.03472*, 2019.
- [14] K. Simonyan and A. Zisserman, “Very deep convolutional networks for large-scale image recognition,” *arXiv preprint arXiv:1409.1556*, 2014.
- [15] J. Ballé, V. Laparra, and E. P. Simoncelli, “Density modeling of images using a generalized normalization transformation,” *arXiv preprint arXiv:1511.06281*, 2015.
- [16] J. Ballé, V. Laparra, and E. P. Simoncelli, “End-to-end optimized image compression,” *CoRR*, vol. abs/1611.01704, 2016. [Online]. Available: <http://arxiv.org/abs/1611.01704>
- [17] A. L. Maas, A. Y. Hannun, and A. Y. Ng, “Rectifier nonlinearities improve neural network acoustic models,” in *Proc. ICML*, vol. 30, no. 1, 2013, p. 3.
- [18] H. Robbins and S. Monro, “A stochastic approximation method,” *Annals of Mathematical Statistics*, vol. 22, pp. 400–407, 09 1951.
- [19] P. Molchanov, S. Tyree, T. Karras, T. Aila, and J. Kautz, “Pruning convolutional neural networks for resource efficient inference,” in *5th International Conference on Learning Representations, ICLR 2017, Toulon, France, April 24-26, 2017, Conference Track Proceedings*, 2017.
- [20] A. Krizhevsky, “Learning multiple layers of features from tiny images,” 2009.